CHARACTERIZATION OF A SPIKING NEURON MODEL VIA A LINEAR APPROACH

by

AMIRHOSSEIN JABALAMELI
B.S. Isfahan University of Technology, 2013

A thesis submitted in partial fulfilment of the requirements
for the degree of Master of Science
in the Department of Electrical Engineering and Computer Science
in the College of Engineering and Computer Science
at the University of Central Florida
Orlando, Florida

Summer Term
2015

Major Professor: Aman Behal

ABSTRACT

In the past decade, characterizing spiking neuron models has been extensively researched as an essential issue in computational neuroscience. In this thesis, we examine the estimation problem of two different neuron models. In Chapter 2, We propose a modified Izhikevich model with an adaptive threshold. In our two-stage estimation approach, a linear least squares method and a linear model of the threshold are derived to predict the location of neuronal spikes. However, desired results are not obtained and the predicted model is unsuccessful in duplicating the spike locations. Chapter 3 is focused on the parameter estimation problem of a multi-timescale adaptive threshold (MAT) neuronal model. Using the dynamics of a non-resetting leaky integrator equipped with an adaptive threshold, a constrained iterative linear least squares method is implemented to fit the model to the reference data. Through manipulation of the system dynamics, the threshold voltage can be obtained as a realizable model that is linear in the unknown parameters. This linearly parametrized realizable model is then utilized inside a prediction error based framework to identify the threshold parameters with the purpose of predicting single neuron precise firing times. This estimation scheme is evaluated using both synthetic data obtained from an exact model as well as the experimental data obtained from *in vitro* rat somatosensory cortical neurons. Results show the ability of this approach to fit the MAT model to different types of reference data.

ACKNOWLEDGMENTS

I would like to express my gratitude to my advisor, Dr. Aman Behal, for his insightful guidance that was so helpful to the work that I have conducted at the University of Central Florida. He was incessantly encouraging, supportive, and ready to provide practical help and advice. I am also grateful to my committee members: Dr. James J. Hickman and Dr. Michael Haralambous.

TABLE OF CONTENTS

LIST OF FIGURES

LIST OF TABLES

CHAPTER 1: INTRODUCTION

As large-scale detailed network modeling projects are appearing in the computational neuroscience area, it becomes essential to construct easily identifiable lower-dimensional models of single neurons. While lower-dimensional models allow for construction of large-scale computational neuronal networks that can be simulated with ease, identifiability of the underlying neuronal models is necessary for the neuronal network to be able to mimic the computational properties of the biological structure being modeled *in silico*. Fortunately, a wide variety of single neuron models are available in literature. These models can broadly be categorized into two main groups: detailed biophysical models and simple phenomenological models, *e.g.,* [1][2]. Detailed biophysical Hodgkin-Huxley [3] type neuron models can accurately reproduce most behaviors of neurons, however, their complex dynamics and a high-dimensional parameter space make them an impractical choice as building blocks for large-scale neuronal networks [4]. In spiking neuron models, since isolated spikes of a given neuron are similar, the shape of the action potential does not represent any information. Instead, it is the spike train, as a sequence of spikes, which is important [5]. Due to this reason and high computational costs, simple phenomenological models such as leaky integrate-and-fire models have been proposed [6][7] and developed to study the dynamics of neural networks [8][1]. Recently, substantial efforts have been put in the expansion of leaky integrate-and-fire models for fitting of such models to data in order to reproduce quantitative features [9][10]. Several methods have been proposed that can accurately predict the timing of spikes, *e.g.*, [11][12][13][14][15].

Identification of model parameters can be performed by several methods. Although hand tuning of parameters may yield reasonable results, this process is labor intensive and impractical. In [4], the versatile quadratic model proposed by Izhikevich [16] was utilized to automatically identify experimentally obtained neuronal firing data. However, as noted in [17], that model cannot be

utilized for identification because it is unable to quantitatively represent the upstroke of the spike unless it is assumed that the model parameters are voltage-dependent [18]. Another proposed model, *viz.*, the Multi-timescale Adaptive Threshold model (MAT) [12] shows great performance for both stationary and non-stationary fluctuating currents to replicate spike trains of experimental data [19]. While the threshold is dependent on five independent parameters, the authors *a priori* fix two time constant related model parameters and identify the other three parameters by maximizing a non-convex performance metric encoding for the coincidence of spikes between the model predictions and the experimental data. Thus, a systematic technique is still needed to automatically identify all five parameters so that the threshold model firing pattern is consistent with that of the experimental data. Furthermore, a convex cost function is needed in order to guarantee parameter convergence. The advantage of such a technique is that it can be utilized in a fully automated system that can identify the underlying neuronal models that are needed to design and implement a realistic biological computational structure. This work focuses on the development of the aforementioned automated identification technique. Specifically, we manipulate the threshold equation into a linear-in-the-parameters model and then proceed to estimate the parameters in order to minimize in a least squares sense the error between the subthreshold voltage and the threshold estimate at the experimentally observed spiking times. Convex constraints are imposed on the optimization to ensure meaningfulness of the obtained parameter estimates. Results show that the proposed scheme outperforms existing strategies in terms of reproducing spike locations. Another novelty of the proposed method is that unlike many other methods that require the input and the reference membrane voltage of the neuron to tune their models, this method only needs the input current and the spike locations to fit the model to the reference data.

The remainder of this thesis is organized as follows. In chapter 2, a modified Izhikevich model is proposed and a two-stage estimation approach is applied to identify the model parameters in order to predict the location of spike times. Next, in chapter 3, the basics of the multi-timescale adaptive

threshold (MAT) model are presented, and a linear-in-the-parameters model with the goal of fitting the MAT model to the reference data is derived. Finally, chapter 4 concludes the thesis.

CHAPTER 2: A MODIFIED IZHIKEVICH MODEL

Introduction

In [16], a second-order model is introduced to be able to reproduce almost all types of firing patterns observed *in-vivo* and keep the computational effort low at the same time. Although the quadratic model is proven to be biological versatile, it can only qualitatively reproduce the firing pattern, *i.e.,* the model cannot quantitatively represent the upstroke of the spike unless assuming voltage-dependent parameters [18]. To address this issue, a modification is made to this model. Instead of assuming voltage-dependent parameters, we remove the quadratic term in the model and make it a representation only for subthreshold dynamics. Since we narrow our interest zone down to the subthreshold region by doing so, problem with the spike upstroke does not affect our identification any more. Another reason to consider simplification of the model instead of making additional assumption is that the modified model dynamics become linear and can be treated analytically.

The rest of this chapter is organized as follows. We begin by proposing a modified Izhikevich model with an adaptive threshold which is assumed to be voltage dependent. In our two-stage estimation approach, first, a linear least squares method is applied to fit the subthreshold model to the reference data and then in the second step, a linear-in-the-parameters model of the threshold is derived to predict the location of neuronal spikes. Finally, we discuss the results obtained from applying the identification procedure to experimental data.

System Model

Original Izhikevich Model

A simple adaptive quadratic spiking model can be described by the state equations [16]

$$\frac{dv}{dt} = k_0 v^2 + k_1 v + k_2 - k_3 (u - i) \tag{2.1}$$

$$\frac{du}{dt} = a(bv - u) \tag{2.2}$$

and the post-spike resetting

$$if\ v = V_p,\ then \begin{cases} v \to c \\ u \to u + d \end{cases}. \tag{2.3}$$

Here, v denotes the membrane potential and is the only system output, u is a membrane recovery state variable which provides a negative feedback to v, while i denotes injected current current. At the peak V_p of the membrane potential, the state variables are reset according to (2.3), c denotes the post-spike reset value of the membrane potential while d denotes the amount of spike adaptation of the recovery variable. The parameters k_3 and a denote the time scale of the two state variables, the parameter b is the level of subthreshold adaptation, while the parameters k_0, k_1, and k_2 are linked to the spike initiation behavior of the neuron. Figure (2.1) shows the variation of the membrane potential and recovery variable at the moment of spike.

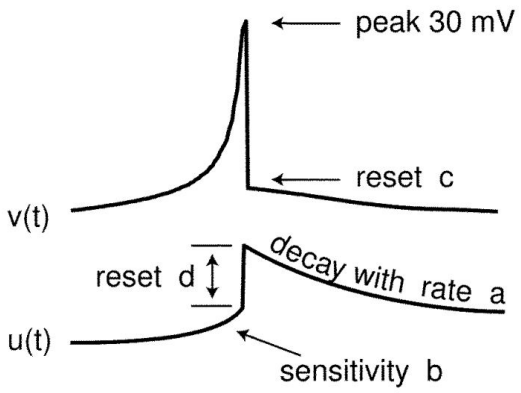

Figure 2.1: Izhikevich Dynamics[1]

Modified Izhikevich Model

Compared to the integrate-and-fire model, the additional variable u, accounting for the activation of K^+ ionic currents and inactivation of Na^+ ionic currents, allows the original model to reproduce many types of firing patterns that are common in biological systems. However, the nonlinearity introduced by the quadratic term does not allow for a facile analytical treatment. Furthermore, variable parameters are needed to reproduce the exact spike shape [18]. To circumvent these difficulties, we remove the quadratic term and present a modified model as follows

$$\frac{dv}{dt} = k_1 v + k_2 - k_3 u + k_3 i \tag{2.4}$$

$$\frac{du}{dt} = a(bu - v). \tag{2.5}$$

Whenever the potential v hits the threshold f, the neuron is said to fire a spike, and the variables are reset according to:

$$if\ v = f,\ then \begin{cases} v \rightarrow c \\ u \rightarrow u + d \end{cases} \tag{2.6}$$

where the symbols retain their earlier definitions. Note that (2.4) and (2.5) only describe the subthreshold approximation, and the post-threshold dynamics of the cell do not form a part of the model, *i.e.,* the upstroke/downstroke are drawn by hand. Unlike [20] in which a triangular pulse is used to mimic the shape of the spike, here, we ignore the whole spiking behavior, only using a straight line to mark the spike arrival. Since the model above is only valid in the subthreshold region, a voltage threshold needs to be defined to indicate the initiation of a spike. A fixed threshold is used by [21]. However, empirical evidence suggests that the voltage threshold for a spike depends not only on the instantaneous value of the voltage, but also on the rate of voltage change which is observed in biological neurons [22]. Thus in this study, motivated by [19], we define the threshold dynamics of the model by considering a term representing the subthreshold voltage-rate dependency and propose the threshold as follows

$$f(t) \triangleq m + k(t) = m + k_v(\frac{dv}{dt}) * \exp(-\lambda t) \tag{2.7}$$

where $*$ denotes the convolution operator, m denotes a dc-offset for threshold voltage that is added to a dynamic threshold function $k(t)$ which is a filtered version of the time derivative of the membrane voltage. The parameter k_v is a coefficient for managing voltage-rate dependency effect on the threshold and λ is the inverse of time constant for the kernel function.

Estimation Procedure

In this section, our goal is to estimate the following set of unknown parameters associated with the proposed model

$$\theta \triangleq (k_1, k_2, k_3, a, b, c, d, m, k_v, \lambda) = (\theta_{s0}, \theta_{t0})$$

where the partitions θ_{s0} and θ_{t0} will be explicitly defined below. It is assumed that the input excitation and membrane potential depolarization recordings are available for measurement. Given the membrane potential trace, it is possible to obtain the spike locations. Given the reduced model, the parameters to be estimated are divided into two sets; specifically, a set $\theta_{s0} \triangleq (k_1, k_2, k_3, a, b)$ which is associated with the linear dynamics of (2.4) and (2.5), and another set $\theta_{t0} \triangleq (c, d, m, k_v, \lambda)$ which is linked to the after-spike resetting and threshold parameters. Thus, the two-stage estimation problem solved in this chapter consists of both matching the subthreshold voltage recording to estimate θ_{s0} and utilizing those estimates as well as the measurements to maximize the performance of the model to predict the spiking pattern to estimate the threshold parameters θ_{t0} .

Subthreshold Estimation (Stage I)

The linear system represented by (2.4) and (2.5) can be analytically treated and solved. In this step, since we only aim to estimate the subthreshold parameters, we drop the resets indicated by 2.6 from the modified model. In fact, by choosing an interval of data, which does not include any spikes in it and is beyond the transient period of a spike, the effect of c and d will be excluded. Therefore, the solution of (2.4) and (2.5) can be utilized to obtain a linear-in-the-parameters model of the subthreshold membrane voltage v. We begin by taking the Laplace transformation of the

model dynamics as follows

$$\begin{cases} sV - v(0) = & k_1 V + + \dfrac{k_2}{s} - k_3 U + k_3 I \\ U = & \dfrac{abV + u(0)}{s+a}. \end{cases} \tag{2.8}$$

Next, by plugging the second row of (2.8) into the first row and rearranging the terms, the sub-threshold dynamics are changed to a single equation:

$$(s+a)(s-k_1)V = -k_3(abV + u(0)) + k_3(s+a)I + (s+a)\frac{k_2}{s} + (s+a)v(0).$$

To avoid the model dependency on the derivatives of the measurement signals, a low pass filter of the form (2.9) is applied to the model representation, and (2.10) is obtained as follows

$$\frac{1}{A} \triangleq \frac{1}{s^2 + \beta_1 s + \beta_0} \tag{2.9}$$

$$\begin{aligned} V = & \frac{[(\beta_1 - a + k_1)s + (\beta_0 + ak_1 - k_3 ab)]}{A} V + \frac{k_3(s+a)}{A} I \\ & + \frac{k_3(s+a)}{A} I + \frac{ak_2}{sA} + [\frac{s}{A} v(0) + \frac{[k_2 - k_3 u(0) + av(0)]}{A}] \end{aligned} \tag{2.10}$$

where s denotes the Laplace variable, V and I represent Laplace transform of v_s and i , and β_1, β_0 are the filter parameters which are considered known during the estimation process. In addition, to reduce parameter dimensionality, the last term of (2.10), which only has transient effects and disappears very fast, is excluded from further calculations. Hence, a compact linear-parameterized

representation of the subthreshold voltage model is provided as follows

$$V = W^T\theta_s = \begin{bmatrix} \frac{sV}{A} \\ \frac{V}{A} \\ \frac{sI}{A} \\ \frac{I}{A} \\ \frac{1}{sA} \end{bmatrix}^T \times \begin{bmatrix} \beta_1 + k_1 - a \\ \beta_0 + ak_1 - k_3ab \\ k_3 \\ k_3a \\ ak_2 \end{bmatrix} \tag{2.11}$$

where $W(v,i) \in R^5$ is a realizable regression vector and $\theta_s \in R^5$ is an unknown parameter vector. Thus, in the subthreshold region, θ_s is only a nonlinear function of θ_{s0} and it is independent of θ_{t0}. Based on the LP model obtained above in (2.11), a prediction error can be defined as follows

$$e_s \triangleq \sum^t (\hat{v}(t) - v(t))^2 = \sum (W^T(t)\theta_s - v(t))^2. \tag{2.12}$$

Among various possible estimation algorithms, we draw up least squares estimation due to its robustness to presence of noise in the system. When the error function is minimized, we obtain

$$2W(t)W^T(t)\hat{\theta}_s = W(t)v(t). \tag{2.13}$$

Therefore, the estimated values for subthreshold parameters is given by

$$\hat{\theta}_s = \sum^t (WW^T)^{-1}(WV). \tag{2.14}$$

In order to obtain the parameters θ_{s0}, a system of equations has to be solved. If we assume the estimated values as a vector which is provided as follows

$$\hat{\theta}_s \triangleq [x_1\ ,\ x_2\ ,\ x_3\ ,\ x_4\ ,\ x_5]^T, \tag{2.15}$$

then the estimated value of θ_{s0} parameters can be calculated by (2.16)

$$\begin{cases} \hat{k}_3 = & x_3 \\ \hat{a} = & x_4/x_3 \\ \hat{k}_2 = & x_5/a \\ \hat{k}_1 = & x_1 + a - \beta_1 \\ \hat{b} = & -(x_2 - \beta_0 - ak_1)/k_3 a \end{cases} \tag{2.16}$$

The convergence of the parameter estimates to their actual values is ensured by utilizing a persistently exciting input current injection. Now, by using the estimated values, it is possible to reconstruct the subthreshold region voltage and employ it in the next steps.

Threshold Estimation (Stage II)

During this stage, first we present the threshold voltage as a linear parametrized (LP) model, then by casting resetting parameters into the subthreshold voltage dynamics, we provide a LP model of subthreshold voltage valid for all times (including spike times). Here, the subthreshold parameters θ_{s0} estimated from the previous step are utilized in the reconstruction of the membrane potential. Based on (2.11), we can explicitly write the dependencies of the reconstructed potential $\hat{v}$ as

follows

$$\hat{v} \ = g(t, i, \hat{\theta}_{s0}, c, d). \tag{2.17}$$

Conditional upon i and $\hat{\theta}_{s0}$, it can be seen that $\hat{v}$ is a linear function of the unknown reset parameters c and d. We remark that in Stage II, the reset parameters (i.e., the initial conditions post spiking) cannot be ignored because these parameters determine the rate of occurrence of spikes. The insight here is that the reconstructed membrane potential is allowed to evolve according to (2.17) and spikes are generated when the reconstructed membrane potential reaches threshold $f(t)$, the unknown parameters $c,\ d,\ m,\ k_v$ and λ are adjusted so as to minimize the error between the estimated membrane voltage and the estimated threshold voltage at the known spike times. During this stage, it is assumed that the the only output measured from the neurons is the location of the spikes. Since the spikes from real neurons have finite width, the spike time t_k is defined to be the time of the peak of each spike. Here, we develop the threshold voltage as a linear-in-the-parameters model as follows

$$f(t) = m + k(t) \Longrightarrow F(s) = \frac{m}{s} + K(s) \tag{2.18}$$

$$K(s) = k_v(s\hat{V} - \hat{v}(0))\frac{1}{s+\lambda} \tag{2.19}$$

By substituting (2.19) into (2.18), we obtain

$$F(s) = \frac{m}{s} + k_v(s\hat{V} - \hat{v}(0))\frac{1}{s+\lambda}. \tag{2.20}$$

To remove the derivative dependency, we apply a first order low pass filter of the form (2.21) in our calculations:

$$\frac{1}{B} \triangleq \frac{1}{s+\eta_0} \tag{2.21}$$

where η_0 is a known filter parameter. Finally, by rearranging the terms, the threshold voltage is given by

$$F\ (s) = \frac{m}{s} + \frac{K(s)}{B}(\eta_0 - \lambda)\ + \frac{k_v}{B}(s\hat{V}(s) - \hat{v}(0)). \tag{2.22}$$

Since $\hat{v}(0)\frac{k_v}{B}$ term only has an initial transient effect, we neglect it from further analysis to reduce parameter dimensionality, and represent the compact form as follows:

$$f(t) = W_t^T\theta_t = \mathcal{L}^{-1}\begin{bmatrix} \frac{1}{s} \\ \frac{K(s)}{B} \\ (\frac{s\hat{V}}{B}) \end{bmatrix}^T \times \begin{bmatrix} m \\ (\eta_0 - \lambda) \\ k_v \end{bmatrix} \tag{2.23}$$

where $W_t \in R^3$ represents a regression vector and θ_t is the unknown parameter vector corresponding to the threshold parameters.

To achieve our goal of estimating neuronal spike times, we integrate the resetting mechanism of the model into (2.4) and (2.5) and make a single equation to introduce the neuron membrane potential. Based on (2.6), the firing happens when voltage v crosses threshold f which instantly resets the voltage to c and the recovery variable jumps by d. Thus, we consider these resets as step functions

that occur at the spike times t_k and develop the model as follows

$$\text{if } v = f \text{ then : } \begin{cases} v \to c \\ u \to u + d \end{cases} \Rightarrow \begin{cases} v \to v + (c - f(t))s(t - t_k) \\ u \to u + ds(t - t_k) \end{cases} \tag{2.24}$$

$$\begin{cases} \dfrac{dv}{dt} = & k_1 v + k_2 - k_3 u + k_3 i + (c - f(t)) \sum\limits_k \delta(t - t_k) - \dfrac{df(t)}{dt} \sum\limits_k s(t - t_k) \\ \dfrac{du}{dt} = & a(bv - u) + d \sum\limits_k \delta(t - t_k) \end{cases} . \tag{2.25}$$

Since we assume that $f\,(t)$ changes slowly with time, $\dfrac{df(t)}{dt}$ is set identically to zero in the above equation. To develop the LP model for the membrane voltage, we follow the same procedure as in the previous section

$$\begin{cases} sV - v(0) = & k_1 V + \dfrac{k_2}{s} - k_3 U + k_3 I + (c - m) \sum\limits_k \exp(-t_k s) - K(s) * \sum\limits_k \exp(-t_k s) \\ SU - u(0) = & abV - aU + d \sum\limits_k \exp(-t_k s) \end{cases} \tag{2.26}$$

where (2.26) indicates the Laplace transformation of (2.25). After rearranging the terms, we obtain a linear-in-the-parameters model for the unknown parameters as follows

$$\begin{aligned} V = \; & \frac{k_2}{sQ(s)} + k_3 \tfrac{I}{Q} - d(\tfrac{k_3}{Q(s)})(\frac{\sum\limits_k \exp(-t_k s)}{s + a}) + \\ & (c - m)\tfrac{1}{Q(s)} \sum_k \exp(-t_k s) - \tfrac{1}{Q(s)}(K(s) * \sum_k \exp(-t_k s)) \end{aligned} \tag{2.27}$$

where $Q(s) \triangleq (s - k_1 + \frac{k_3 ab}{s+a})$ represents a filter which is used for simplifying the notation. Motivated by our desire to predict the spike times of a neuron, in this stage, we design our objective

function according to mechanism of generating spikes in the proposed model. Since the firing happens when $v(t)$ and $f(t)$ take same values, the objective is to minimize their difference at the spike times. Therefore, the error function is given by

$$e_t = \sum^{t_k} (\hat{f}(t) - \hat{v}(t))^2 \tag{2.28}$$

where $\hat{f}(t) \triangleq W_t^T \hat{\theta}_t$ while $\hat{v}(t)$ has been previously defined in (2.17). By replacing the threshold and membrane voltage LP models from (2.23) and (2.27) into the (2.28), one can obtain a linear objective function with respect to the unknown parameters as follows

$$E_t(s) = \sum^{t_k} (W^T(s)\hat{\theta} + M(s))^2 \tag{2.29}$$

$$W^T(s)\hat{\theta} = \begin{bmatrix} \frac{1}{\hat{Q}} \sum \exp(-t_k s) \\ -\frac{\hat{k}_3}{\hat{Q}} (\frac{1}{s+\hat{a}}) (\sum \exp(-t_k s)) \\ -\frac{1}{\hat{Q}} \sum \exp(-t_k s) - \frac{1}{s} \\ \frac{K_0}{B} \\ -\frac{1}{B}(s\hat{V}_s) \end{bmatrix}^T \times \hat{\begin{bmatrix} c \\ d \\ m \\ \lambda \\ k_v \end{bmatrix}} \tag{2.30}$$

$$M(s) = \frac{\hat{k}_2}{s\hat{Q}} + \hat{k}_3 \frac{I}{\hat{Q}} - \frac{1}{\hat{Q}} (K_0(s) * \sum_k \exp(-t_k s)) - (\eta_0)\frac{K_0}{B} \tag{2.31}$$

where $\hat{Q}(s) \triangleq (s - \hat{k}_1 + \frac{\hat{k}_3 \hat{a} \hat{b}}{s+\hat{a}})$, $W(s)$ is a regression vector, while $M(s)$ is an auxiliary signal dependent on the estimated parameters from stage I. Since the objective function is a quadratic

function of the unknown parameters, the minimizing solution is given as follows (2.32).

$$\hat{\theta} = -\sum^{t_k}(WW^T)^{-1}(WM). \tag{2.32}$$

Note that the existence of solution for $\hat{\theta}$ is dependent on the invertibility of the WW^T signal.

Implementation

In our simulations, the excitation is done with the current generated from an Ornstein–Uhlenbeck process [2]. The total injected current $I(t)$ is given by

$$I(t+dt) = I(t) - \frac{I(t)}{\tau_I}dt + m_I dt + s_I \zeta(t)\sqrt{dt} \tag{2.33}$$

where m_I and s_I are parameters and $\zeta(t)$ is a zero-mean, unit variance Gaussian random variable. The process was generated and injected at a rate of 5 kHz ($dt = 0.2\ ms$) and the correlation length τ_I was $1\ ms$. The resulting current $I(t)$ has a stationary Gaussian distribution with mean $\mu_I = m_I\tau_I$ and variance $\sigma_I^2 = s_I^2\tau_I/2$.

Although no iterative procedure is apparent at first glance when utilizing (2.14) and (2.32), the dependence of the signal K_0 in (2.30) on k_v and λ (unknown parameters which we are trying to estimate) forces us to utilize an estimate of K_0 computed using estimates of k_v and λ from the previous step instead and apply the algorithm iteratively until all parameters converge. To summarize, the 2-step estimation problem is solved via the following iterative procedure:

- Step 1: Estimate subthreshold parameters using Eq. (2.14).
- Step 2: Generate estimated subthreshold voltage with Step I estimated parameters based on

(2.4) and (2.5).

- Step 3: Initialize the threshold algorithm by selecting starting parameters k_{v0} and λ_0.
- Step 4: Estimate the threshold and resetting parameters.
- Step 5: If the threshold parameters have converged, stop the process, otherwise update the threshold parameters and go to Step 3.

Results and Discussion

We applied the aforementioned two-stage estimation strategy to the reference data which was generated in the *NEURON [23]* simulation environment by using an ion-channel based spiking model [24]. First, we applied the stage I estimation process to the subthreshold region. Figure (2.2) indicates the predicted subthreshold voltage using estimated parameters. According to the obtained results, the subthreshold traces are very close to each other, showing that dynamics (2.4) and (2.5) yield good approximation in the linear zone. In the next step, the θ_{s0} set is used to estimate for the resetting and threshold parameters. In this stage, estimated values for θ_{t0} were utilized to generate spike locations based on the proposed model; however, desired results were not obtained and the predicted model was unsuccessful in duplicating the spike locations. Possible reasons for this failure could lie in the choice of (a) the stimulating current, (b) subthreshold model, (c) threshold model, and/or (d) error functions. Further investigation is needed to zero in on the exact reasons for the failure to obtain useful results via this approach.

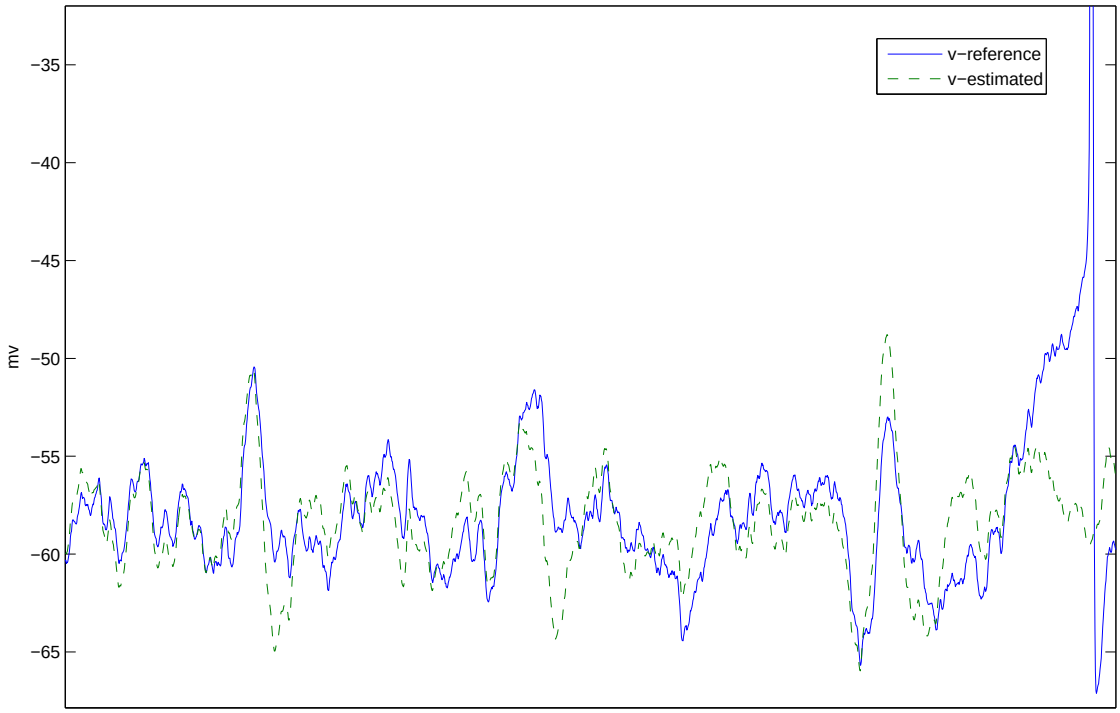

Figure 2.2: Subthreshold estimation

CHAPTER 3: A MULTI-TIMESCALE ADAPTIVE THRESHOLD MODEL

Introduction

This chapter is organized as follows. In Section II, we first present the basics of the multi-timescale adaptive threshold (MAT) model. Next, in Section III, we pursue the mathematical manipulations and the proposed scheme to identify the MAT model parameters. The implementation procedure is described in Section IV. In Section V, results are provided on model identification from different types of reference data. Relevant conclusions are drawn in Section VI.

The MAT Model

The Multi-timescale Adaptive Threshold (MAT) model [12] was proposed by Kobayashi *et al.* for the purpose of predicting the timing of output spikes of neurons. The MAT model can be described by a subthreshold voltage V and a multi-timescale adaptive threshold f. While it is possible in general to have an arbitrary number of timescales, the analysis in this paper will be limited to two timescales as similarly done in [12]. The subthreshold voltage can be obtained by the leaky integrator which is given by a first order differential equation (3.1)

$$\tau_m \frac{dV}{dt} = -V(t) + RI(t) \tag{3.1}$$

where $V(t)$ denotes a membrane potential, $I(t)$ is the injected input current, while τ_m and R are parameters that describe leaky time constant and input resistance, respectively. While Equation (3.1) is the foundation of Generalized Linear Models and Spike Response Model [5], however, in

the MAT model, the variable $V(t)$ is not reset after reaching a constant or time/state dependent threshold. Instead, at the spiking instants defined by the intersection of V and f, the threshold variable f resets to a different value in the manner shown below

$$f(t) = \alpha_1 \sum^{t_k} \exp(-k_1(t - t_k)) + \alpha_2 \sum^{t_k} \exp(-k_2(t - t_k)) + \omega \tag{3.2}$$

where t_k is the k^{th} spike time, k_1 and k_2 denote inverses of the two threshold time constants, α_1 and α_2 denote the increments of the threshold at the spike instants, while ω is the threshold resting value. Furthermore, an absolute refractory period τ_R is defined to prevent consecutive firing; consequently, within τ_R period after a spike, the model cannot fire more spikes even if the subthreshold voltage is above the threshold. As seen in Figure (3.1), spikes (represented by arrows) are assumed to be generated whenever the subthreshold voltage reaches the threshold voltage from below. The moment of crossing is the so-called firing time at which instant the threshold voltage increases a certain amount and then starts decaying exponentially to its resting value.

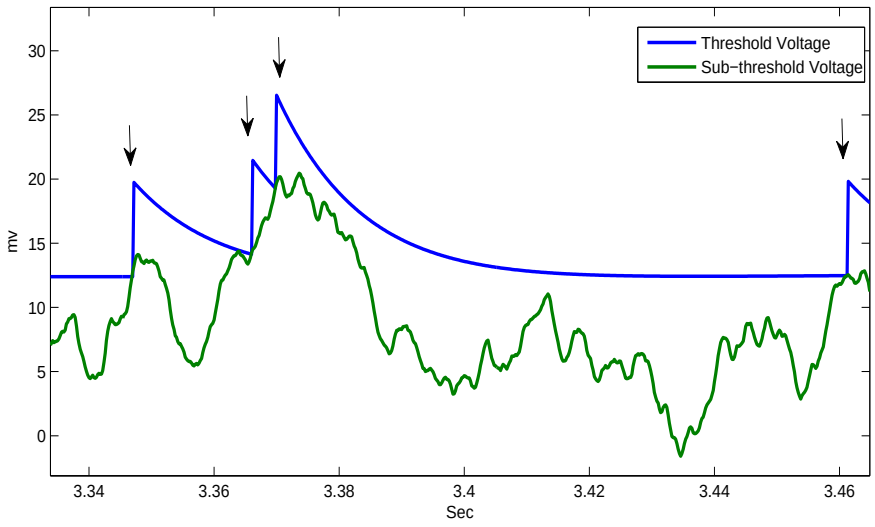

Figure 3.1: Dynamics of the MAT model. When the threshold voltage (blue) intersects the sub-threshold voltage (green), a spike is generated and the threshold increases.

The Proposed Estimation Technique

Pursuant to the development in section 2, the MAT model can be completely characterized by 7 free parameters; where $\{\tau_m, R\}$ are the leaky integrator parameters and $\{\alpha_1, \alpha_2, k_1, k_2, \omega\}$ are the spike threshold parameters. The resistance R does not affect the spike time prediction and only scales the subthreshold voltage [12]; furthermore, a common membrane time constant (τ_m) is extracted from the data and preselected for all simulations. Therefore, we focus our work to estimate the threshold parameters and we assert that $\theta_0 \triangleq [\alpha_1, \alpha_2, k_1, k_2, \omega]^T$ completely describes the model. In what follows, we develop an automatic method for estimating the MAT model parameters.

Linear Parametrization

While the static threshold representation of (3.2) is nonlinear with respect to the parameters k_1 and k_2, a dynamic representation can be developed to acquire a linearly parameterized model. By taking Laplace transform of (3.2) and rearranging the terms, one can obtain

$$\begin{aligned}(s^2)F(s) = \; & -[(k_1+k_2)\,s + k_1k_2]F(s) + [(\alpha_1+\alpha_2)\,s \\ & + (\alpha_1k_2+\alpha_2k_1)]\sum^{t_k}\exp(-t_ks) \\ & +[ws^2 + w\,(k_1+k_2)\,s + wk_1k_2]\tfrac{1}{s}\end{aligned} \tag{3.3}$$

where s is the Laplace variable and $F(s)$ represents the Laplace transform of $f(t)$. A second order low pass filter

$$\frac{1}{A} = \frac{1}{s^2+\beta_1 s+\beta_0} \tag{3.4}$$

is employed in order to eliminate the model dependency on derivatives of the measurable signals [4]. The following can be obtained by applying the filter to both sides of (3.3):

$$\begin{aligned}F(s) = \; & (\tfrac{\beta_1 s+\beta_0}{A})F(s) - (k_1+k_2)\,\tfrac{s}{A}F(s) - k_1k_2\tfrac{1}{A}F(s) \\ & + (\alpha_1+\alpha_2)\,\tfrac{s}{A}\sum^{t_k}\exp(-t_ks) + (\alpha_1k_2+\alpha_2k_1) \\ & \underbrace{\tfrac{1}{A}\sum^{t_k}\exp(-t_ks) + wk_1k_2\tfrac{1}{A}\tfrac{1}{s}+}_{[w\frac{s^2}{A}\frac{1}{2} + w\,(k_1+k_2)\,\frac{s}{A}\frac{1}{s}]}\end{aligned} \quad . \tag{3.5}$$

Since the last row of (3.5) vanishes beyond an initial transient, we can neglect it in the subsequent calculations to reduce the dimension of the parameter vector. Ultimately, the linearly parameterized (LP) model is described as follows

$$f(t) = \Psi^T(f,t,t_k)\theta + \Phi(f,t) \tag{3.6}$$

where $\Phi(f,t)$ is a signal that is independent with respect to the model parameters and $\Psi(f,t,t_k) \in \mathbb{R}^5$ is a regression vector. These signals are defined as follows

$$\Phi(f,t) \triangleq L^{-1}\left\{(\frac{\beta_1 s+\beta_0}{A})F(s)\right\} \tag{3.7}$$

$$\begin{aligned}\Psi(f,t,t_k) \triangleq \quad & L^{-1}[\tfrac{s}{A}F(s), \tfrac{1}{A}F(s), \tfrac{s}{A}\sum^{t_k}\exp(-t_k s), \\ & \tfrac{1}{A}\sum^{t_k}\exp(-t_k s), \tfrac{1}{sA}]^T\end{aligned} \tag{3.8}$$

while $\theta \in \mathbb{R}^5$ is an unknown auxiliary parameter vector that is a nonlinear function of θ_0 and defined as follows

$$\theta = [-(k_1+k_2), -k_1k_2, \alpha_1+\alpha_2, \alpha_1k_2+\alpha_2k_1, wk_1k_2]^T. \tag{3.9}$$

Development of Constrained Least Squares Algorithm

According to the MAT model process, firing happens whenever the subthreshold voltage reaches the threshold voltage. In other words, $f(t)$ and $V(t)$ are equal at the spike instants. Since the main objective in this work is to fit the MAT model to the reference data in order to obtain a predictive model for the location of spike times, we define a prediction error variable as follows for each spike moment

$$e_{t_k} \triangleq \hat{f}(t_k) - V(t_k) \tag{3.10}$$

where $\hat{f}\ (t)$ denotes an estimate of $f(t)$. A natural cost function based on the prediction error for all spike instants can be defined as

$$J \triangleq \sum^{t_k} e_{t_k}^2$$

and developed as follows

$$J = \sum^{t_k} (\hat{f}(t) - V(t))^2 = \sum^{t_k} (\Psi(f, t, t_k)\hat{\theta} + \Phi(f, t) - V(t))^2 \tag{3.11}$$

based on the LP model derived in (3.6). Here, $\hat{\theta}$ denotes an estimate for θ. Therefore, the objective is to find the MAT model parameter that minimize the prediction error

$$\hat{\theta} = \arg\min \left\{ J = \sum^{t_k} (f(t) - V(t))^2 \right\} \tag{3.12}$$

However, certain constraints need to be introduced so that the parameter estimates $\hat{\theta}$ converge to physically meaningful values when mapped back to the actual parameter space θ_0. The actual model parameters can be obtained in closed form as follows

$$k_1 = \max(\frac{-\theta_1 \pm \sqrt{\theta_1^2 + 4\theta_2}}{2}) \tag{3.13}$$

$$k_2 = \min(\frac{-\theta_1 \pm \sqrt{\theta_1^2 + 4\theta_2}}{2}) \tag{3.14}$$

$$\alpha_1 = \frac{\theta_4 - k_1\theta_3}{k_2 - k_1}\ ,\ \alpha_2 = \theta_3 - \alpha_1\ , w = \frac{-\theta_5}{\theta_2} \tag{3.15}$$

where θ_i denotes the i^{th} component of θ. While there are no restrictions on α_1, α_2, and w other than that they are real (which is trivially enforced), k_1 and k_2, being time constants, are needed by the model to be positive and real. Thus, the set of equations above suggest the inequalities

$$\theta_1, \theta_2 < 0 \text{ and } \theta_1^2 + 4\theta_2 \geq 0 \tag{3.16}$$

to ensure the real positiveness of k_1 and k_2. As seen in Figure 3.2, these inequalities define a non-convex region. Since k_1 and k_2 denote different timescales, a separation based on available data

and studies suggests the choice $20 \leq k_1 \leq 500$, $2 \leq k_2 \leq 20$ (the unit is $1/\sec$). Based on this feasible range, the following set of convex constraints can be obtained

$$\begin{gathered} -520 \leq \theta_1 \leq -22, -10^4 \leq \theta_2 \leq -40 \\ 38.5\theta_1 - \theta_2 \leq -1482 \\ -1.7\theta_1 + \theta_2 \leq 0 \end{gathered} \tag{3.17}$$

which is a triangular area demarcated in Figure 3.2 by the dashed blue and green lines and the vertical solid black line.

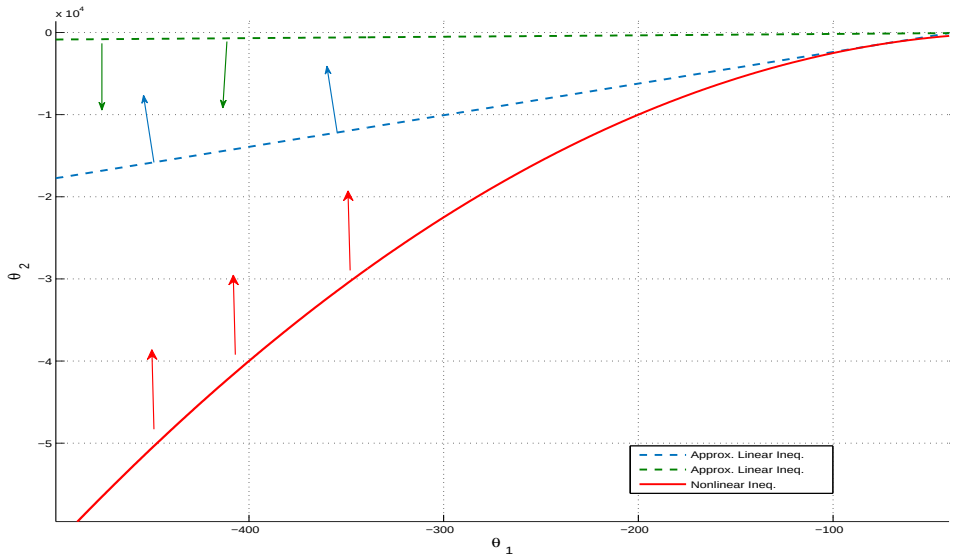

Figure 3.2: Feasible Region for Solution

The above set of constraints does not preclude intersection of V and f between the experimentally observed spiking instants as shown in Figure 3.3. However, it is impractical to check for and enforce this condition at all times. Instead, we endeavor to enforce this constraint practically by observing the maximum value of $V(t)$ between each pair of spikes and corresponding instant t_m

following which we enforce the following convex constraint between each pair of spikes:

$$f(t_m) - V(t_m) = \Psi^T(t_m)\theta + \Phi(t_m) - V(t_m) > 0. \tag{3.18}$$

This constraint essentially states that the subthreshold voltage at its peak between any pair of experimentally observed spikes is not allowed to cross over the threshold. Of course, this does not preclude intersection altogether since the threshold is time varying but it is an easily implementable set of constraints that serves well to improve the model efficacy by reducing false positives as will be seen in the sequel.

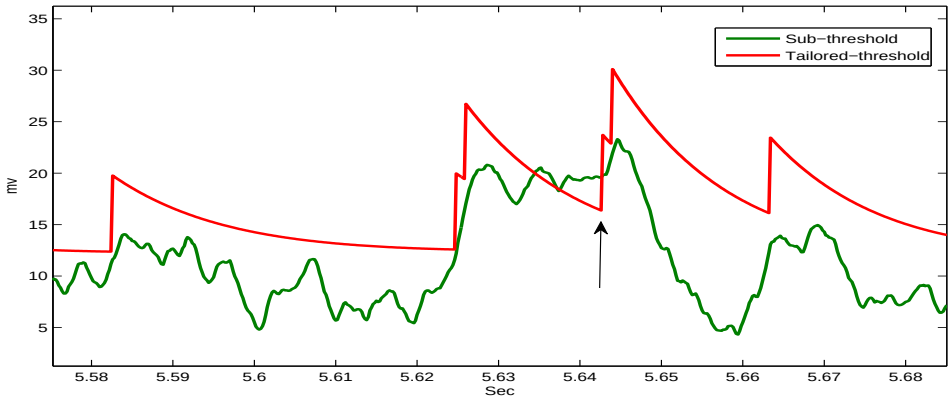

Figure 3.3: Per the objective function, the method only minimizes the error at the spike times without considering intersections of subthreshold (green) and threshold voltage(red) between spike times.

Implementation Procedure

Although no iterative procedure is apparent at first glance when solving the constrained least squares problem defined by (3.12), (3.17) and (3.18), the unavailability of the signal f in (3.11)

forces us to utilize $\hat{f}$ instead and apply the algorithm iteratively until the parameters converge. The implementation proceeds according to the following steps:

Step 1: Generate subthreshold voltage V: Since the objective function (3.12) requires sub-threshold voltage V, we solve (3.1) by assuming $R = 50M\Omega$ and $\tau_m = 5\ ms$. Following [2], the excitation is performed with current generated from an Ornstein–Uhlenbeck process as follows

$$I(t + dt) = I(t) - \frac{I(t)}{\tau_I}dt + m_I dt + s_I \zeta(t)\sqrt{dt} \tag{3.19}$$

where m_I and s_I are parameters and $\zeta(t)$ is a zero-mean, unit variance Gaussian random variable. In our simulations, the process is generated and injected at a rate of 5 kHz ($dt = 0.2\ ms$) and the correlation length τ_I is $1\ ms$. The resulting current $I(t)$ has a stationary Gaussian distribution with mean $\mu_I = m_I\tau_I$ and variance $\sigma_I^2 = s_I^2\tau_I/2$.

Step 2: Build signals $\Psi(\cdot)$ and $\Phi(\cdot)$ by using (3.7) and (3.8): Since both are dependent on f which is not available for measurement, we begin with an initial guess $\hat{\theta}_0$ for θ_0 and build $\hat{f} \triangleq f(\hat{\theta}_0, t, t_k)$ based on which we build $\hat{\Psi}(\cdot) \triangleq \Psi(\hat{f}, t, t_k)$ and $\hat{\Phi}(\cdot) \triangleq \Phi(\hat{f}, t)$. During estimation computations, $f(t)$ does not reset at the times where the threshold crosses the subthreshold, instead, the generated $f(t)$ fires at the reference (experimentally obtained) spike times, t_k.

Step 3: Minimize the objective function (3.11) to obtain $\hat{\theta}$ subjects to the set of constraints (3.17) and (3.18). The loop error is defined as follows:

$$e(\hat{f}) \triangleq \sum^{t_k} (\Psi(\hat{f}, t, t_k)\hat{\theta} + \Phi(\hat{f}, t) - V(t))^2 \tag{3.20}$$

where $e(\hat{f})$ denotes the error of $\hat{f}$ that is generated by $\hat{\theta}$ at the end of the loop. Since the error function is a quadratic function of variables which is subject to linear constraints on those variables, the optimization problem (3.12) at each step is formulated as a Quadratic Programming problem.

Step 4: Solve $\hat{\theta}$ to obtain $\hat{\theta}_0$ according to (3.13)-(3.15).

Step 5: Finally, $\hat{\theta}_0$ is updated at Step 2 with new parameters and the procedure is repeated until all parameters converge to constant values.

Evaluation of Prediction

The error function defined in (3.11) is useful for estimating parameters but it cannot be an evaluation criterion since the main aim of this work is to predict the spike train produced by the neurons. While the firing rate of a spike train provides helpful information, yet, the evaluation of similarity between two spike trains is needed to capture local artifacts. Several measures exist for comparing the spike train predicted by the model and the spike train generated by the reference data. A popular index known as the *coincidence factor* has been proposed in [2]. The coincidence factor Γ measures both the similarity and dissimilarity of two spike train by considering the spiking rate and coincident spikes. Γ is calculated as follows

$$\Gamma = \frac{N_{Coinc} - \ < N_{Coinc} >}{N_{Data} + N_{Model}} \times \frac{2}{1 - 2\upsilon\Delta} \tag{3.21}$$

where N_{Data} is the number of spikes in the reference spike train, N_{Model} is the number of spikes in the predicted spike train, N_{Coinc} is the number of coincidences with precision Δ between the two spike trains, and $< N_{coinc} >$ is the expected number of coincidences generated by a homogeneous Poisson process with the same rate υ as the spike train of the model. The factor $2/(1 - 2\upsilon\Delta)$ normalizes Γ to a maximum value of 1 which is reached if and only if the spike train of the model reproduces exactly the reference spike train. Hence, after identifying the model parameters, we calculate the value of the Coincidence Factor to evaluate the predicted spike times.

Results and Discussion

In this section, the parameters of the MAT model are identified by the proposed method to match three types of reference data: (a) data from the MAT model, (b) noisy version of data from the MAT model, and (c) experimental data. The synthetic datasets are used to test validity and robustness of our approach. For our experimental data, we utilized a standard dataset from a Quantitative Neuron Modeling competition [2] which includes the excitation input and single-electrode data recorded from a cortical pyramidal neuron in slices of rat barrel cortex. The details of the experimental protocol are available in [25] and [26]. The injected input current is generated based on (3.19) and stimulation is done with currents of different means and fluctuation amplitudes. Additionally, for computing Coincidence Factor, the value of Δ is set to $2\ ms$, since it is in the same range as the accuracy of measuring synaptic rise times in the soma of cortical pyramidal neurons [2].

Results from MAT Reference Data

First, to show the ability of the proposed method to identify the model parameters, a reference train of spikes is produced by the exact MAT model using a known set of parameters shown in Table (1). The subthreshold voltage V is generated via the method described in Section 3 and is assumed to be noiseless. For the reference data generation, the parameters for the model are chosen arbitrary and pointed out in Table (1). The initial guess for θ_0 is chosen as follows

$$\alpha_1 = 10 \quad \alpha_2 = 5 \quad k_1 = 50 \quad k_2 = 8 \quad \omega = 13$$

Following the procedure in Section 3, the parameters are seen to converge to final values as shown in Table (3.1). It is seen that the estimated values are very close to the actual model parameters. Figures (3.4) and Fig. (3.5) represent the convergence of the objective function value and the esti-

mated parameters along the estimation loops. To illustrate the evolution of the threshold function, Figure (3.6) shows the generated $f(t)$ in a few sample process loops.

Table 3.1: Identified and Actual Parameters for The MAT Reference Data

θ_0	α_1	α_2	k_1	k_2	ω
Identified Val.	3.93	0.48	98.39	4.71	15.13
Actual Val.	4	0.5	100	5	15

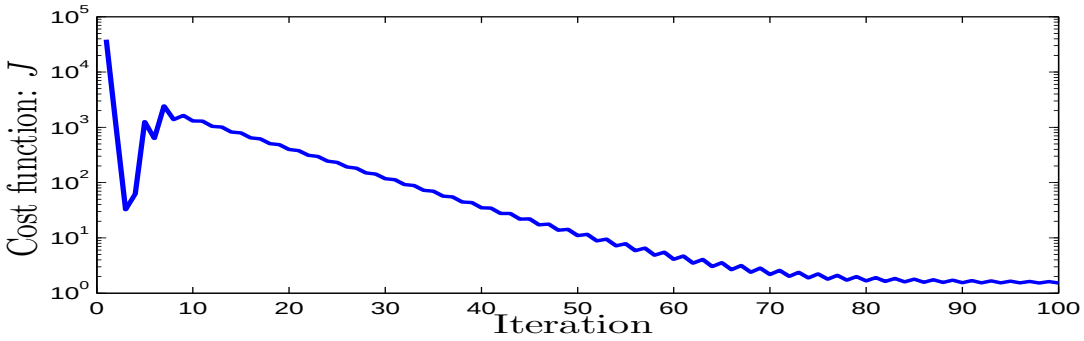

Figure 3.4: Objective function error. The vertical axis is log scale and indicates the value of the error function along the estimation loops

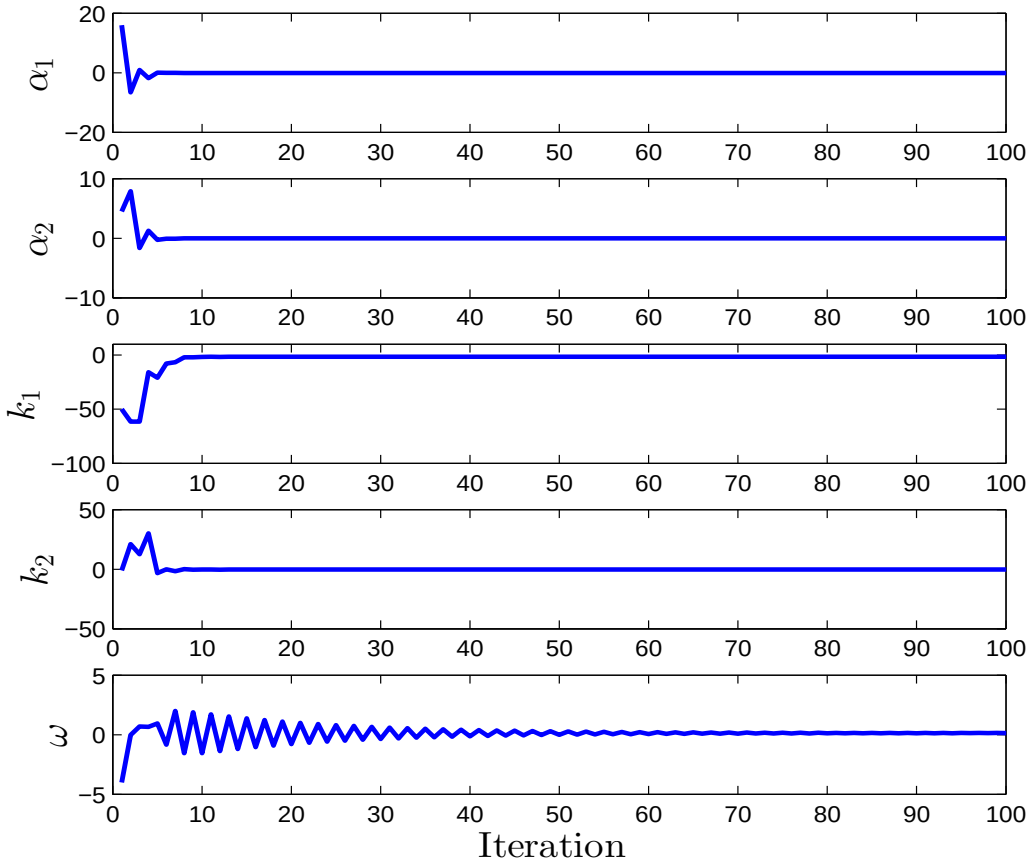

Figure 3.5: Error of the parameters. The diagrams show variation of the parameters $\alpha_1, \alpha_2, k_1, k_2$ and ω during the estimation loops.

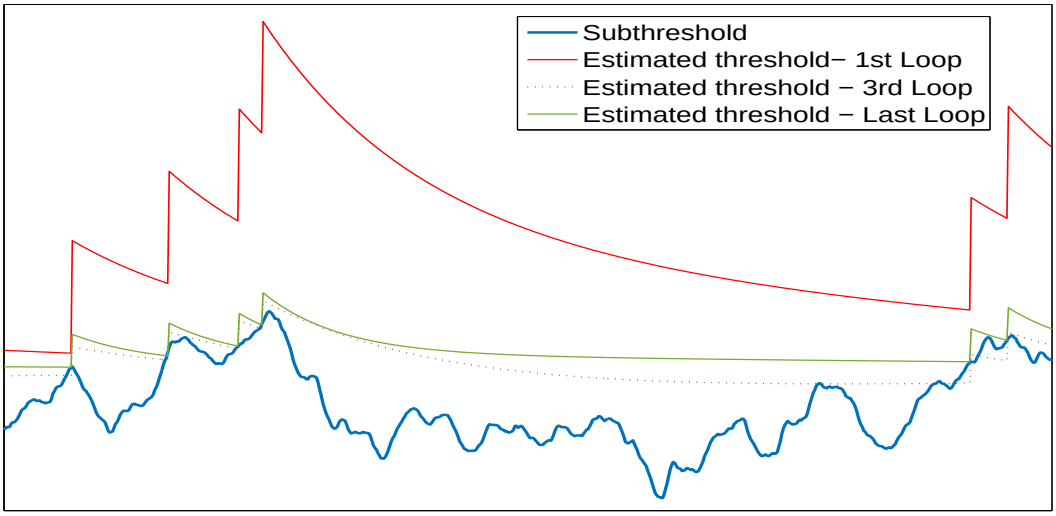

Figure 3.6: Convergence of estimated threshold during the loops

Results from Noisy MAT Reference Data

In a neural recording experiment *in vivo,* the input current received by the neuron is divided into two components, a deterministic one and a stochastic [5]. The deterministic part does not vary during the trials with the same stimulus and the stochastic part represents all the remaining inputs which change during the trials. Therefore, to consider noise in the biological system, the stochastic component of the input is treated as noise which is added to the right hand side of the subthreshold voltage dynamics. Specifically, we modified the subthreshold voltage by adding Gaussian White Noise and the simulations were performed for different SNR values to measure robustness of the proposed method against noise. Our simulations show that the randomness of the generated noise causes the parameters to not converge during some trials. Table (2) describes the obtained results for 10 trials of performed simulations. It is seen that the rate of non-convergence and the average

error per spike over the converged trials ($\bar{e}$) decreases as SNR becomes better.

Table 3.2: Estimation Results for The Noisy MAT Model Reference Data

	$SNR = 40$	$SNR = 35$	$SNR = 30$
Convergence	$8/10$	$7/10$	$5/10$
$\bar{e}$	0.0273	0.0502	0.1669

Results from Experimental Data

After confirming the ability of the proposed method to identify the exact model reference data, the estimation procedure is applied to *in vitro* experimental data. We first present a sample set of data provided by the Single Neuron Competition (data#1, Challenge A, 2007). The identified parameters for the input current (0.62$\pm$0.34 nA) and the corresponding spike train are presented in Table (3).

Table 3.3: Identified Parameters for The Experimental Reference Data

θ_0	α_1	α_2	k_1	k_2	ω
data#1	15.4	-1.49	76	11.6	33.5

After the identification process, the estimated parameters were utilized in a MAT model to predict the spike train. Obtained results for comparing the reference spike train and predicted spike train are shown in Table (4) for two data samples (data#2 and data#11). Figure (3.7) displays the experimental trace and predicted MAT model voltages (for data#11) while the similarity of the spike trains is pointed out by the spike times.

Table 3.4: Comparison of The Predicted Spike Train Similarity and Reference Spike Train

	N_{Data}	N_{Model}	N_{Coinc}	Γ
data#2	268	246	230	0.88
data#11	212	162	144	0.76

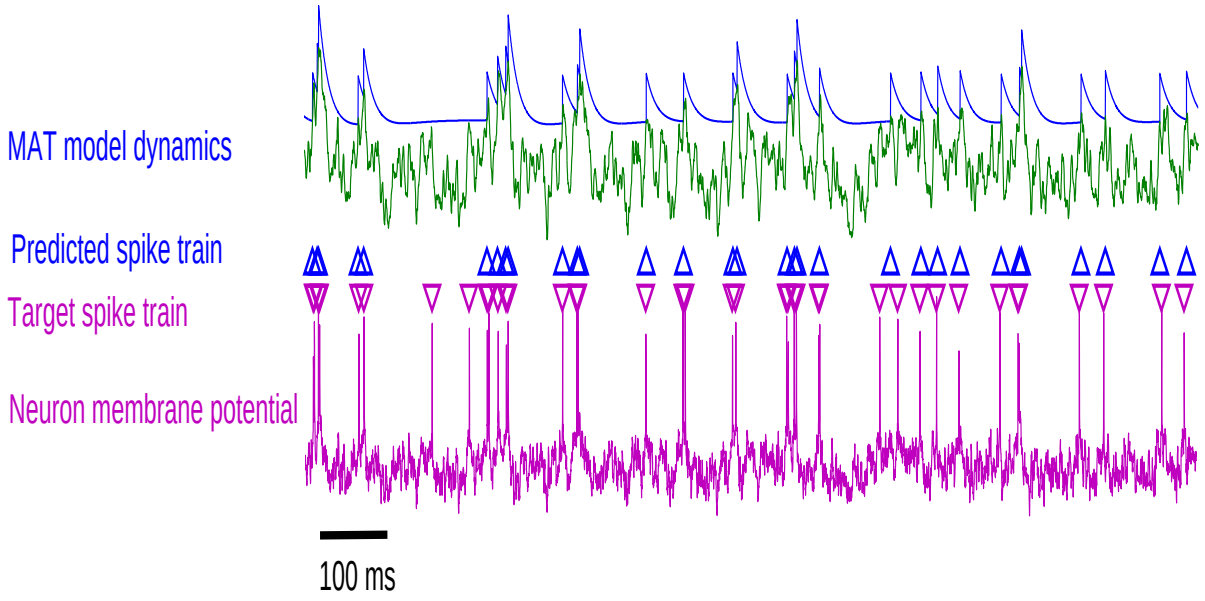

Figure 3.7: Model prediction for fluctuating current according to the experimental data. The top row is the subthreshold (green) and threshold (blue) voltages trace of MAT model, where predicted spike times are specified by blue triangles. The bottom row, indicates the experimental membrane potential (magenta) from a single neuron, where the actual spike train are marked by magenta triangles.

As discussed earlier in the paper, a set of intersection constraints is applied to the objective function per (3.18). To clarify the contribution of these intersection constraints, comparisons were made between spike trains predictions from models estimated with and without the use of constraints.

Table (5) shows the comparative results using an experimental data sample. It can be seen that the use of constraints increases the accuracy of predicting spike times by more than 20%. In fact, the intersection constraints drive the estimator to avoid undesirable spikes and as a result the firing rate is decreased. Although unconstrained estimator predicts higher percentage of target spikes correctly, its performance, represented by coincidence factor, is worse than the constrained one.

Table 3.5: Comparison of Predicted Spike Train for Unconstrained/Constrained Estimation

	Unconstrained	Constrained
N_{Coinc}/N_{Model}	% 69	% 92
N_{Coinc}/N_{Data}	% 88	% 51
Spikes / sec	176	77
Γ Coinc. Fac.	0.35	0.59

In [27], a benchmark test was established to facilitate a systematic comparison of methods and models in predicting the activity of rat cortical pyramidal neurons. The provided data set includes four different input currents which were generated based on (3.19). For each injected current, four trials were recorded to observe if the neuron fires with high reliability. To evaluate the quantitative predictive feature of our approach, we compare our proposed method performance with the benchmark test reported results. Fig. (3.8) indicates the average performance of our method along with the benchmark test results on the whole data set. The raw $\bar{\Gamma}$ is computed by averaging the values of Γ over the whole test set. Since for a certain input, the pyramidal neuron is more reliable than for the others [28], the normalized Γ_A is also introduced. Γ_A scales the raw Γ according to reliability of the neuron which is evaluated with trial-to-trial variation of the neuron recordings [12]. Of the four submissions for the challenge, the auto regressive method (AR) demonstrated the best performance. The AR method uses a mathematical model to estimate the membrane potential of the neuron and then the spike times were predicted by adjusting a dynamic threshold to the estimated membrane potential. The parameters of this model were determined so that the coincidence factor

Γ would be maximized. The carbon-copy method (CC) also yielded a good performance; however it does not benefit from any mathematical model. The CC method utilizes the mean and variance of fluctuating current and evokes a sequence of spike by considering the training data set. There were also two other anonymous submissions in the challenge whose performances are presented here. It is seen that the proposed method is superior to the challenge submissions by both the $\bar{\Gamma}$ and the Γ_A metrics.

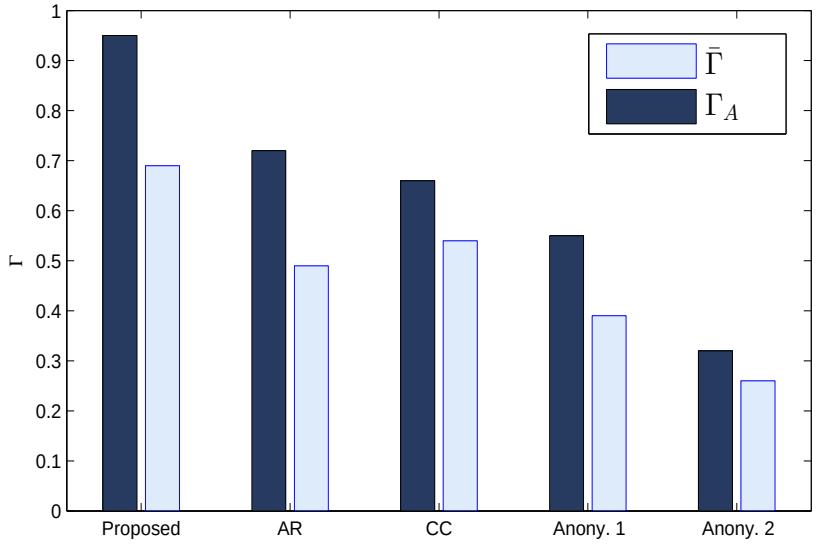

Figure 3.8: Comparison of the proposed method to results of the challenge.

Discussion

In this study, we took advantage of the MAT model which comprises two dynamics. Although the simplified subthreshold leaky integrator dynamics fail to consider many aspects of neuronal dynamics [5], the leaky integrator free parameters provide adequate strength to track the neuron membrane potential trace. Furthermore, the threshold dynamic of MAT model makes effective use

of its multi-timescale feature. Biologically speaking, the multiple timescales can be regarded as surrogates for ionic currents such that different timescale values represent fast transient current, non-inactivating current, *etc.* [19].

The proposed linear representation of the MAT model along with the novel objective function and constraints provides a framework for fitting the model to a single neuron recording in order to predict the quantitative features. The results for prediction of reference data generated from the exact MAT model confirm the validity of the manipulated equations and demonstrate the ability of the approach to find the best parameters even in the presence of noise. While the obtained results from experimental data demonstrate a high performance in predicting reference spike times, a detailed discussion is merited to analyze our approach more clearly. Our utilization of the objective function of (3.12) clarifies that the defined error function does not have an inherent mechanism to consider the non-spike moments. To overcome this issue, we added innovative constraints in our estimation procedure to control the threshold voltage from potential intersections with the subthreshold voltage during the period between two spikes. As shown above, the application of the constraints allows the identified model to generate the spike train with more confidence such that, by avoiding potential false positives, the firing rate is reduced which in turn leads to a higher predictive performance.

To evaluate of the proposed approach, we also compared the predictive performance of our identified model to the submissions for Quantitative Neuron Modeling. Our results show the superiority of the proposed linear method to predict reference spike trains. In addition to improvements in prediction, our method benefits from a convex cost function while at least some of the other submissions in the challenge utilize the non-convex Γ Coincidence Factor as the cost function to maximize their prediction performance. Thus, our proposed approach also has a lower computational cost and a guaranteed global minimum which further underscores its superiority among the other methods. Finally, an obvious deficit of the MAT model is its inability to respond appropriately to

rectangular and ramp currents. Therefore, future work will focus on model modification so it can response to not only fluctuating currents but also different input types.

CHAPTER 4: CONCLUSION

In chapter 2, a modified Izhikevich model was proposed by removing the quadratic term from the original Izhikevich model and a new spike generation mechanism was drawn. A linear-in-the-parameters model was developed to represent the subthreshold dynamics as well as the threshold voltage. Then, a two-stage estimation algorithm was utilized to identify the subthreshold and threshold parameters. The obtained results indicate that our method has the ability to estimate the subthreshold voltage, however, it was unable to predict spike locations for a variety of possible reasons as discussed.

In chapter 3, we proposed a constrained linear least squares algorithm to identify MAT model parameters, for predicting single neuron spike times. Our results show that the proposed identification method is robust to system noise and has the ability to find the best parameters to replicate the spike train. Moreover, the obtained experimental results indicates that our method has excellent performance in comparison to reported results from the Quantitative Neuron Modeling competition [2].Convexity of the cost function is another advantage when compared with similar fitting approaches utilized by the neural community. While the MAT model succeeds in reproducing quantitative features of single neurons, it still lacks the capability to replicate different firing patterns; hence, there is room to investigate possible modifications of the model in the future.

LIST OF REFERENCES

[1] E. M. Izhikevich. Which model to use for cortical spiking neurons. IEEE Trans. Neural Networks 15:1063–1070, 2004.

[2] R. Jolivet, F. Schurmann, T.K. Berger, R. Naud, W. Gerstner and A. Roth. The quantitative single-neuron modeling competition. Biol. Cybern. 99, pp. 417–426, 2008.

[3] A.L. Hodgkin, A.F. Huxley. A quantitative description of membrane current and its application to conduction and excitation in nerve. J Physiol-Lond, 117, pp. 500–544, 1952.

[4] L. Zhi, J. Chen, P. Molnar and A. Behal. Weighted least-squares approach for identification of a reduced-order adaptive neuronal model. IEEE Trans. on Neural Networks and Learning Systems, vol. 23, no. 5, pp. 834-840, May 2012.

[5] W. Gerstner, W. M. Kistler, R. Naud and L. Paninski. Neuronal dynamics: From single neurons to networks and models of cognition. Cambridge University Press, Cambridge, 2014.

[6] N. Brunel, M.C. van Rossum. Lapicque's 1907 paper: from frogs to integrate-and-fire. Biol Cybern 97: 337–339, 2007.

[7] R. B. Stein.A theoretical analysis of neuronal variability. Biophys.J. 5, 173–194. 1965.

[8] W. Gerstner, W. M. Kistler. Spiking neuron models. Cambridge University Press, Cambridge, 2002.

[9] A. Prinz, C. Billimoria, and E. Marder. Alternative to hand-tuning conductance-based models: Construction and analysis of database of model neurons. J. Neurophysiol. vol. 90, pp. 3998-4015, Aug. 2003.

[10] Q.J.M. Huys, M.B. Ahrens, L. Paninski. Efficient estimation of detailed single-neuron models. J Neurophysiol, 96, pp. 872–890, 2006.

[11] R. Jolivet, W. Gerstner.Predicting spike times of a detailed conductance-based neuron model driven by stochastic spike arrival. J Physiol-Paris 98(4–6):442–451, 2004.

[12] R. Kobayashi, Y. Tsubo, and S. Shinomoto.Made-to-order spiking neuron model equipped with a multi-timescale adaptive threshold. Front.Comput.Neurosci. 3:9. doi:10.3389/neuro.10.009, 2009.

[13] R. Kobayashi,and S. Shinomoto. State space method for predicting the spike times of a neuron. Phys.Rev.E 75, 011925, 2007.

[14] C. Clopath, R. Jolivet, A. Rauch, H. R. Lüscher, W. Gerstner. Predicting neuronal activity with simple models of the threshold type: Adaptive exponential integrate-and-fire model with two compartments. Neurocomputing 70(10–12):1668–1673, 2007.

[15] B. Shahrasbi, A. Talari, and N. Rahnavard. TC-CSBP: Compressive Sensing for Time-Correlated Data Based on Belief Propagation. Annual Conference on Information Sciences and Systems, 2011.

[16] E. M. Izhikevich. Simple model of spiking neurons. IEEE Trans. Neural Networks 14:1569-1572, Nov. 2003.

[17] J. Chen, J. Suarez, P. Molnar, and A. Behal. Maximum likelihood parameter estimation in a stochastic resonate-and-fire neuronal model. *1^{st} IEEE International Conference on Computational Advances in Bio and Medical Sciences*, Orlando, FL, pp. 57-62, February 2011.

[18] E. M. Izhikevich. Dynamical systems in neuroscience: The geometry of excitability and bursting. The MIT Press, 2007.

[19] S. Yamauchi, H. Kim, S. Shinomoto. Elemental spiking neuron model for reproducing diverse firing patterns and predicting precise firing times. Front. Comput. Neurosci. 5:42 10.3389/fncom.2011.00042 , 2011.

[20] R. Jolivet, T. J. Lewis, W. Gerstner, "Generalized Integrate-and-Fire Models of Neuronal Activity Approximate Spike Trains of a Detailed Model to a High Degree of Accuracy," *J. Neurophysiol* vol.92, pp. 959-976, 2004.

[21] E. M. Izhikevich, "Resonate-and-fire Neurons," *Neural Networks*, vol. 14, pp 883-894, 2001.

[22] R. Azouz, C. M. Gray., "Dynamic Spike Threshold Reveals a Mechanism for Synaptic Coincidence Detection in Cortical Neurons *in vivo*, " *Proc. Natl. Acad. Sci. USA*, vol. 97, pp. 8110-8115, 2000.

[23] M.L. Hines and N.T. Carnevale, "The NEURON simulation environment", Neural Computat. 9: 1179–1209, 1997.

[24] D. A. McCormick, Z. Wang, J. Huguenard, "Neurotransmitter Control of Neocortical Neuronal Activity and Excitability," Cereb Cortex. vol. 3, pp. 387-398. 1993.

[25] A. Rauch, G. La Camera, H.R. Lüscher, W. Senn, S. Fusi. Neocortical pyramidal cells respond as integrate-and-fire neurons to in vivo-like input currents. J Neurophysiol, 90, pp. 1598–1612, 2003.

[26] G. La Camera, A. Rauch, D. Thurbon, H. Lüscher, W. Senn, S. Fusi. Multiple time scales of temporal response in pyramidal and fast spiking cortical neurons. J Neurophysiol, 96, pp. 3448–3464, 2006.

[27] R. Jolivet, R. Kobayashi, A. Rauch, S. Shinomoto and W. Gerstner. A benchmark test for a quantitative assessment of simple neuron models. J. Neuroscience Methods 169, pp. 417–424, 2008.

[28] Z. Mainen, T. Sejnowski. Reliability of spike timing in neocortical neurons. Science, 268, pp. 1503–1506, 1995.